# Zinc oxide nanostructured films produced via anodization: A rational design approach

**Anyela Ramirez-Canon,[a] David Miles,[a] Petra Cameron,[b] and Davide Mattia[c*]**

Nanostructured zinc oxide films were produced through anodization of zinc foil by using different electrolytes at different voltages, temperatures and over different time periods. The ZnO films were characterised by studying their surface morphology using FESEM, crystal structure using XRD, wetting behaviour through contact angle measurement, and also measuring the profile of the ZnO layer and band gap. Results show that the type of electrolyte and its concentration determine the morphology and size of the nanostructures. Voltage, time and temperature affect the distribution and density of the nanostructures along the surface. The band gaps of the films were in the range of 3.27 to 3.50 eV. Although ZnO is a hydrophilic material, some of the films display hydrophobic and super-hydrophobic behaviour. The data obtained in this study was combined with literature studies and used to devise design guidelines to obtain ZnO films with specific nanostructures and macroscopic properties by controlling the anodization parameters.

## Introduction

Zinc oxide (ZnO) exhibits a promising combination of a direct band gap of 3.37eV, piezoelectric properties and high stability of excitons.[1,2] The former makes ZnO a potential candidate for light emission applications,[3] whilst the combination of the other properties is useful to develop optoelectronic and sensor devices.[4–6] In terms of its photocatalytic properties, ZnO has been widely studied for different uses, such as self-cleaning paints,[7] cosmetics, sun creams and for the photo-degradation of organic molecules.[8]

Several techniques for the production of nanostructured ZnO films have been reported in the literature, including chemical vapour deposition,[9,10] epitaxial growth,[11] electrodeposition,[12] and anodization.[13–17] Through these methods diverse nanostructures such as nanowires, nanorings, nanoflakes, nanoneedles, nanocages and nanospheres have been produced.[18] Although different studies on the production of zinc oxide nanostructures using these methods have been carried out, the mechanism that controls the shape and sizes of nanostructures is still not well understood.

Among these techniques, anodization holds great promise in that it allows a large variety of morphologies to be obtained. Through this electrochemical process it is also possible to control the size and density of the nanostructures by modifying the type of electrolyte, voltage, temperature and reaction time. Some of the nanostructures obtained through different studies by anodizing Zn include: nanoporous-like structures,[12] nanoflakes,[13,19] microtip,[16] stripe-like nanostructures,[18] nanocrystals,[21] nanoparticles,[22] nanoflowers,[23] nanoneedles,[23,24] and nanowires.[20,25,26] Although some preliminary work to understand the effect of experimental conditions on the structures' morphology has been done, there has been no systematic investigation of the effect of voltage, temperature, electrolyte type and concentration, and reaction time on film morphology, with several publications looking only at particular sub-sets of each parameter.[15,20] Furthermore, only few of these studies have included analysis of mechanical, optical, and surface properties.[21]

In this study a systematic comparative analysis was carried out by producing ZnO nanostructured films using six different electrolytes, two of which have not yet been reported in the literature. The effect of voltage, temperature, reaction time and electrolyte concentration on the morphology of ZnO nanostructures was studied. The wetting behaviour, crystallinity and band gap of the obtained films were also investigated. Some of the obtained films showed hydrophobic and super-hydrophobic behaviour. Hydrophobicity has been attributed to high surface roughness and to low surface energy.[15] The hydrophobicity of ZnO nanostructures obtained through hydrothermal synthesis[27] and magnetron sputter deposition has been reported previously,[28–31] However, ZnO super-hydrophobic surfaces obtained by anodization have not been reported before. The results obtained in this study have been correlated to the synthesis parameters, leading to formulation of rational design guidelines for ZnO nanostructure formation via anodization.

## Experimental

### Synthesis

ZnO nanostructured films were produced using an anodization method. High purity zinc foil (99.98%, 0.25mm thickness, Alfa Aesar) was cut into pieces of 1.0 cm by 1.5 cm and used as the starting material. In a typical experiment, the zinc foil was annealed in air at 300 °C (CWF1100, Carbolite) for one hour, followed by a cleaning process with acetone (HPLC grade, 99.5+%, Fisher) in an ultrasonic bath for 10 minutes. Before anodization, the samples were electro-polished by applying 20 V for 15 minutes in an electrolyte solution of ethanol (>99.8%, Sigma Aldrich) and perchloric acid (60-62 %, Alfa Aesar) in a volumetric ratio of 1:2. Anodization was performed in a 2-electrode cell with 8 mm spacing, using the electropolished zinc foil as the anode and stainless steel (SS316 grade) as the cathode. Different types of ethanolic solutions were used as electrolytes i.e. orthophosphoric acid ($H_3PO_4$, 85%, Alfa Aesar), nitric acid

($HNO_3$, 65%, Sigma Aldrich), hydrochloric acid (HCl, 37% solution, Acros Organic), oxalic acid ($H_2C_2O_4$, 98%, Acros Organic), sodium hydroxide (NaOH, 1M volumetric solution, Fisher), and an aqueous solution of potassium bicarbonate ($KHCO_3$, 99.99% Powder, Sigma Aldrich). For each electrolyte, the electrochemical experiments were carried out at two different voltages (1 V and 40 V) provided by a DC power supply (Agilent E3634A); two concentrations of electrolyte (0.1M and 1M) and time (1 minute and 1 hour). The temperature of the electrolyte was kept constant throughout anodization (0 °C or 10 °C) using a water cooled bath (Thermo Scientific). Once anodization was complete, the samples were thoroughly rinsed with ethanol and deionized water and dried for 36 hours in a vacuum desiccator at $2x10^{-3}$ mbar (Bio Rad – Microscience Division). Subsequently, the films were stored in a desiccator cabinet for further analysis.

**Characterization**

The surface morphology of each film was observed using a JEOL 6301F field emission scanning electron microscope (FESEM) and a JEOL JSM6480LV scanning electron microscope (SEM) equipped with an energy dispersive X-ray spectrometer (EDX, Oxford, ONCA x-ray analyser, Oxfordshire, UK). The wetting behaviour was examined by means of contact angle measurement using an Optical Contact Angle Measuring device with automatic dosing system (OCA-5, Dataphysics, Gerhard UK). A 2µL drop of deionised water was dropped on the surface and contact angles were measured at 3 different points for each film. The crystal structure was studied using an X-ray diffraction system (Philips Xray generator – PW 1710 diffractometer) set in flat plate mode and the measurements were carried out between 2θ values of 0° and 100°. Band gap measurements were obtained by measuring the UV-visible absorbance spectra of the ZnO films using a UV-visible photospectometer (Ocean Optics, USB2000+UV-VIS, Florida, USA) set in reflectance mode, using electro-polished Zn foil as a blank. Profiles of the ZnO surface were acquired using a surface profiler (Veeco Metrology – Dektak 6M) set with a range of 2620 KÅ and a length of 1000µm.

**Data Analysis**

The main parameters in the anodization of Zn are the type and concentration (*C*) of the electrolyte, the applied voltage (*V*) across the cell, the temperature (*T*) of the electrochemical bath and the anodization time (*t*). A parametric analysis combining the ZnO nanostructures developed in this work and those from previous literature studies was conducted to elucidate which combination of *C*, *V*, *T* and *t* will give a certain nanostructure. Although temperature affects the morphology of the formed nanostructures, a large number of publications have reported this parameter only as 'room temperature'; as such, it was not possible to include temperature effects in all of the analysis. As different types of electrolytes at different concentrations have been used in the literature, the pH of those solutions has been measured to offer a common analysis framework.

For the morphology analysis, ZnO nanostructures developed in this work and those already published in the literature have been classified in six groups as follows:

- smooth – no nanostructure
- pitting – corrosion
- aligned arrays of 1D nanostructures– nanowires, nanoneedles, nanorods
- 2D – nanoplatelets, nanoflakes
- 3D arrangement – interpenetrated nanostructures

For the wetting behaviour analysis, results of contact angles of the ZnO films obtained were classified into three large groups:

- Hydrophilic surface (Contact angle < 90°)
- Hydrophobic surface (Contact angle ≥ 90° and ≤ 120°)
- Super-hydrophobic surface (Contact angle > 120°)

For the profile analysis, ZnO films were classified as follows:

- ZnO layer predominantly concave
- ZnO layer predominantly flat
- ZnO layer predominantly convex

The results are shown in graphical form and guidelines are provided in the results section. The graphical analysis of the data was processed using MATLAB® 11 software.

## Results and Discussion

**Structure and morphology**

As a result of the anodization process, the formation of a white layer of ZnO on the Zn foil occurred. Its composition was confirmed by Energy Dispersive X-ray analysis (EDX). The crystallinity of the films obtained was examined by XRD. Results show that films obtained after anodization, with no post-annealing treatment, contain a combination of amorphous and crystalline ZnO (Fig. S1a). Post-annealing treatment results in increasing crystallinity which is in agreement with other studies involving postannealing treatment on nanostructures (Fig. S1b).[32] For the latter, XRD patterns revealed a wurtzite crystal structure. The strong intensity of the signal from the 002 plane in all samples indicates a strong orientation of the crystal to the c-axis direction. XRD patterns showed also a strong peak on the plane 101 for ZnO, However this peak corresponds mainly to the plane 002 for Zn where these two planes overlap. Similar results have been reported for ZnO nanostructures obtained with different electrolytes.[14,22,26]

During anodization, two competing processes resulted in the formation of ZnO nanostructures: the first was the formation of a Zn ion ($Zn^{2+}$) and further oxidation to ZnO; simultaneously, the newly formed ZnO is re-dissolved in solution. Tuning of the anodization parameters allowed control of the two processes, leading to the presence or absence of nanostructures and, in the former case, control over their morphology and properties.[33,34] The general reaction scheme for the anodization of zinc can be represented as follows:

Anodization

At the cathode:

$$2H^+ + 2e^- \rightarrow H_2(g) \quad (1)$$

At the anode:

$$Zn \rightarrow Zn^{2+} + 2e^- \quad (2)$$

$$Zn^{2+} + 2OH^- \rightarrow Zn(OH)_2 \quad (3)$$

$$Zn(OH)_2 \rightarrow ZnO + H_2O \quad (4)$$

Dissolution

$$ZnO + HX^* \rightarrow ZnX^* + H_2O \quad (5)$$

ZnO films showed different profiles that vary from convex to concave (Figure 1). These profiles are formed as a result of competition between oxide formation and dissolution, suggesting

also that the growth of the nanostructures is not homogeneous along the Zn foil surface, and potential external factors such as stirring can also affect the formation of the ZnO layer.

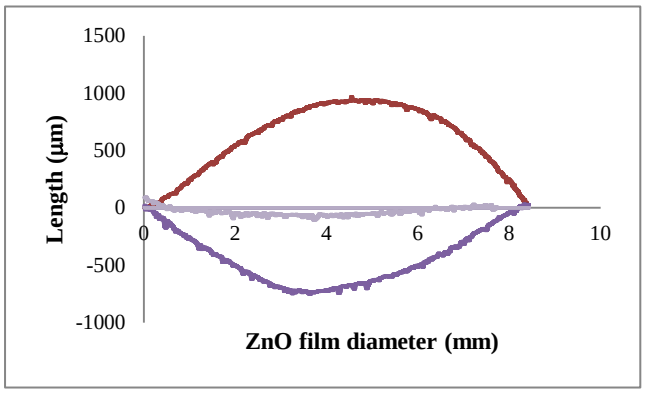


**Fig 1.** Surface profile of ZnO films produced at different anodization conditions: Convex profile (red line) film obtained using $HNO_3$ (0.1 M, 1 V, 1 min, 10 °C); flat profile (lilac line) film obtained using $H_2C_2O_4$ (0.1 M, 40 V, 1 min, 10 °C); concave profile (purple line) film obtained using $H_3PO_4$ (0.1 M, 1 V, 60 min, 10 °C).

**Effect of the type and concentration of electrolyte on film morphology**

Figure 2 displays the FESEM micrographs of the film surfaces obtained in this study for different electrolytes. These suggest that the shape of the nanostructures is determined mainly by the type of electrolyte used and its concentration. Flake-like nanostructures were obtained using $H_3PO_4$; nano-flower-like structures were obtained using HCl, NaOH, $H_2C_2O_4$, and $HNO_3$; nanorods and nanowires were obtained with $KHCO_3$ as the electrolyte. Nanostructures with the largest sizes were obtained using $KHCO_3$ and $HNO_3$ at 0.1 M with an average size of 100 nm, whilst the smallest nanostructures were found in the films obtained using NaOH and $H_3PO_4$, also at low concentration (0.1M).

Concentration plays an important role in the final size of the nanostructure: A high concentration of electrolyte involves a higher concentration of the zinc ion ($Zn^{2+}$) and a high concentration of hydroxyl groups ($OH^-$) available for producing ZnO (Eq.s 2 and 3). Low concentrations lead to the formation of well-defined nanostructures while higher concentrations result in denser nanostructures and, therefore, thicker ZnO layers are produced. For all electrolytes investigated increasing the concentration results in a higher surface density of nanostructures (Figure 3).

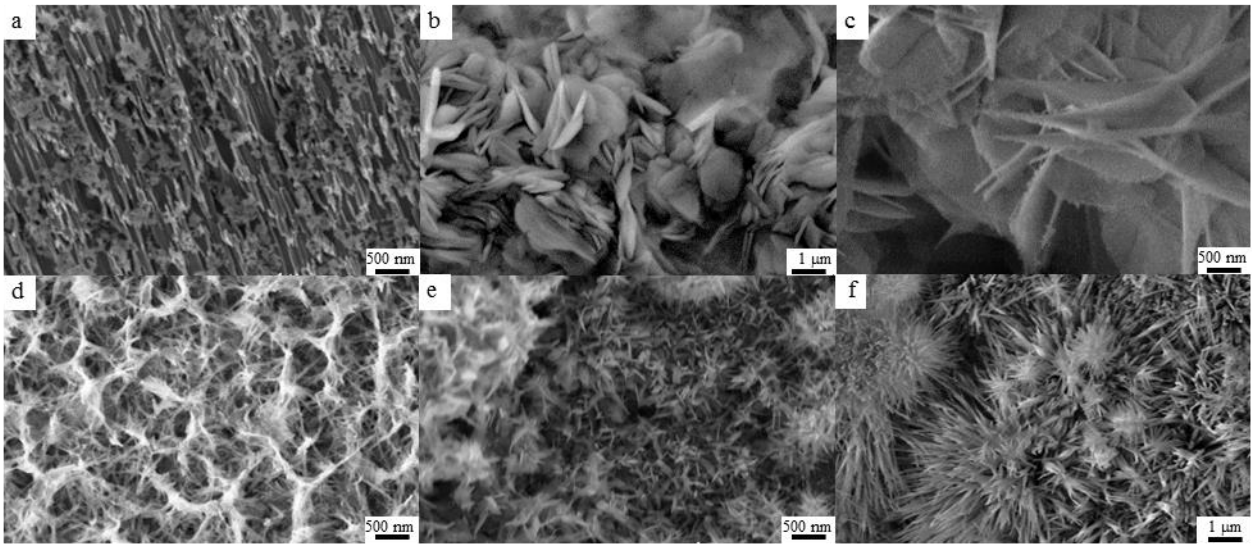


**Fig 2.** SEM micrographs of morphologies obtained with different electrolytes: a) $H_3PO_4$ (1 M, 40 V, 1 min, 10 °C); b) $HNO_3$ (1 M, 1 V, 1 h, 10 °C); c) HCl (0.1 M, 40 V, 1 h, 10 °C); d) $H_2C_2O_4$ (0.1 M, 1 V, 1 h, 10 °C); e) NaOH (0.1 M, 40 V, 1 h, 10 °C); f) $KHCO_3$ (1 M, 1 V, 1 h, 10 °C)

**Effect of voltage on film morphology**

Similarly to the effects of high concentration, a high voltage (40 V) leads to an increase in the concentration of $Zn^{2+}$ during anodization and, therefore, a higher production rate of ZnO than at low voltage (1 V), resulting in dense nanostructures (Figure 4). The increase in nanostructure surface density can be observed by comparing the films obtained at 1 V to those obtained at 40 V for 0.1M (Figure 4a, 4b, and 4c) or 1M (figure 4d). This phenomenon is more pronounced for films produced with $HNO_3$, NaOH and HCl.

For $H_2C_2O_4$ and $H_3PO_4$, the use of a high voltage resulted in pitting of the ZnO layer even at a low concentration. For $KHCO_3$, an anodization voltage of 40 V leads to formation of linked or interpenetrated structures. From SEM observations, it is speculated here that these structures might be the result of nanowires bending beyond a certain length and tangling with adjacent wires. This phenomenon might not occur with other electrolytes due to significantly shorter length of the formed nanostructures.

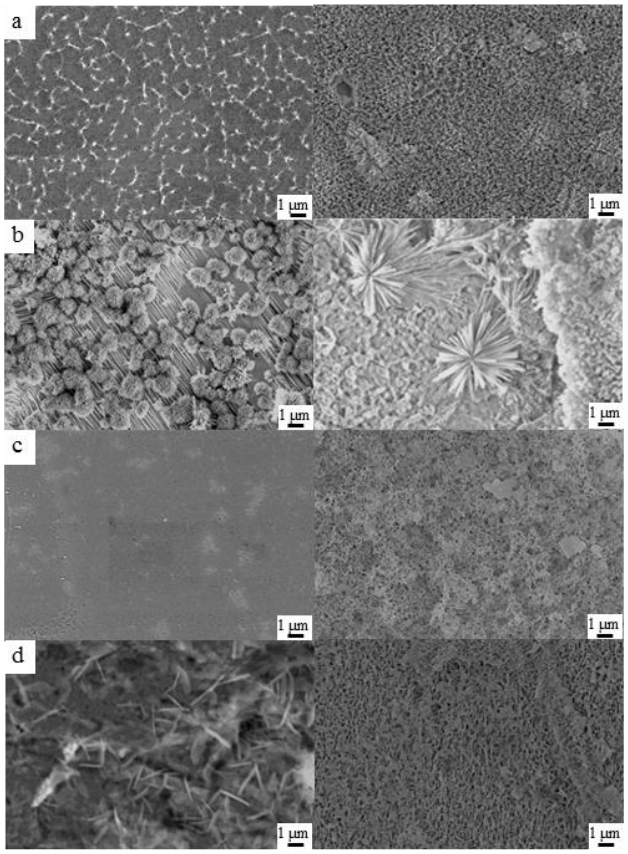


**Fig 3.** SEM micrographs of morphologies obtained at 1 V, 10 °C, for 1 minute, with different electrolytes at 0.1 M (left) and 1 M (right): a) $H_2C_2O_4$; b) $KHCO_3$; c) $H_3PO_4$; d) HCl.

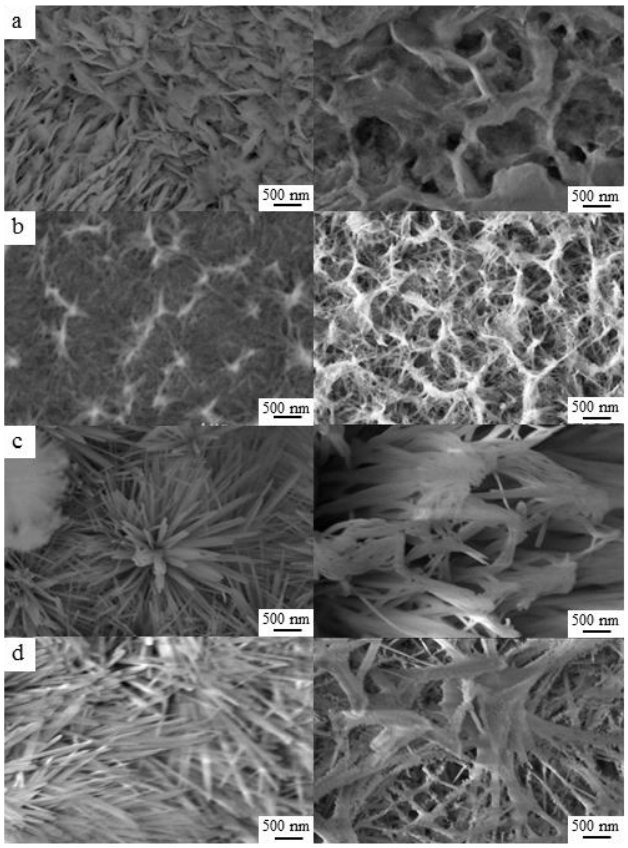


**Fig 4.** FESEM Images of morphologies obtained at 10 °C, for 1 hour, with different electrolytes at two different voltages 1 V (left) and 40 V (right): a) $KHCO_3$ (0.1M); b) HCl (0.1M); c) NaOH (0.1M); d) $KHCO_3$ (1M).

**Effect of temperature on film morphology**

In general the influence of temperature varies between electrolytes. For acidic electrolytes, temperature appears to have a significant effect on the nanostructure morphology only for low values of the anodization voltage and electrolyte concentration. For higher values of voltage, concentration and time, the influence of these parameters is predominant over temperature. Films obtained with $H_3PO_4$ at 0 °C showed dense morphologies without well-defined structures. Anodization with $HNO_3$ at low voltage (1 V) and low temperature (0 °C) resulted in a modest increase in the amount of nanostructures per unit area, with smaller sizes compared to those produced at 10 °C. However, at high voltage no significant differences were observed. Temperature does not have a significant influence on nanostructures obtained with NaOH at 1 V, but at 40 V the reduction of temperature results in an almost featureless surface. Low temperature (0 °C) anodization with HCl electrolyte resulted in the formation of denser morphologies with non-homogenous nanostructures shapes. Similar morphologies were obtained at 0 °C and 10 °C with $C_2H_2O_4$. Films obtained at 0 °C with $KHCO_3$ and 1V are comprised of thicker nanowires than those produced at 10 °C. However, at high voltage it appears that the etching process dominates, leading to the complete dissolution of the Zn substrate.

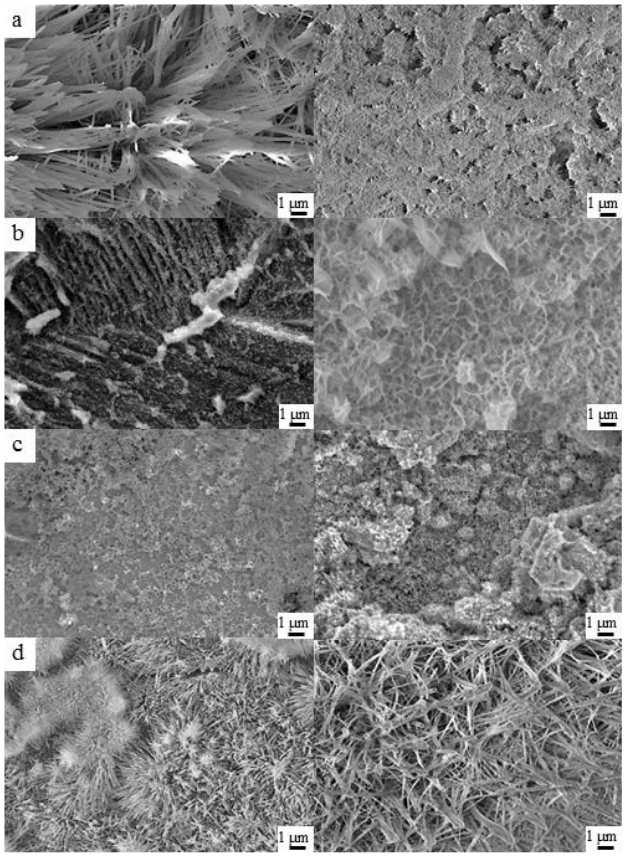


**Fig 5.** SEM micrographs of morphologies obtained at 10 °C and over two different time periods: 1 minutes (left) and 60 minute (right): a) HCl (1 M, 1 V); b) $H_2C_2O_4$ (0.1 M, 1 V); c) $KHCO_3$ (0.1 M, 1 V); d) $KHCO_3$ (1 M, 40 V).

**Effect of time on film morphology**

The effect of the anodization time on the morphology is more complex: In general nanostructures produced over a longer time period are denser. This effect is the result not only of each feature

growing larger but also of a structuring of those features, with the formation of 3D interpenetrated structures (Figure 5). This effect is more pronounced at higher electrolyte concentrations, where there are more $Zn^{2+}$ ions available, as discussed earlier.

**Wetting Behaviour**

Contact angles measured in this study varied from 20º to 157º (± 2º). Nanorods and nanowires obtained with $KHCO_3$ showed the highest contact angles values with a maximum of 152º and a minimum of 125º. This result agrees with other studies in which nanorod-like structures produced by different methods also exhibited hydrophobic and super-hydrophobic behaviour.[31] High contact angles (> 120º) were also obtained with other electrolytes at certain conditions, i.e. $H_3PO_4$ (0.1 or 1 M, 40V, 1 h, 0 °C; $HNO_3$ (0.1 or 1 M, 1 V, 1 min 10 °C); HCl (0.1 or 1 M, 1 or 40 V, 1 h, 10 °C); NaOH (0.1 M, 40 V, 0 or 10 °C).

Given the large variety of structures of the ZnO films produced, their wetting behaviour can be analysed using the Cassie-Baxter and Wenzel models (Figure 6).[35,36] Nanostructures with a high aspect ratio, such as those obtained with $KHCO_3$ (Figure 6a) are assumed to behave according to the former model, with air trapped between the vertically aligned structures. Lower aspect ratio structures tend to have lower contact angles, though still in the hydrophobic and super-hydrophobic range, following Wenzel's model (Figure 6b – 6d). Smaller, less organized or less well-defined nanostructures, on the other hand, exhibit low contact angles, closer to the value for smooth ZnO films.[24]

Contact angle values were maintained when measurements were repeated on samples stored in a dry box for several days. On the other hand, samples left in air exhibited a substantial decrease in the measured contact angle due to the absorption of humidity form the atmosphere, as observed for other ZnO super-hydrophobic structures.[32]

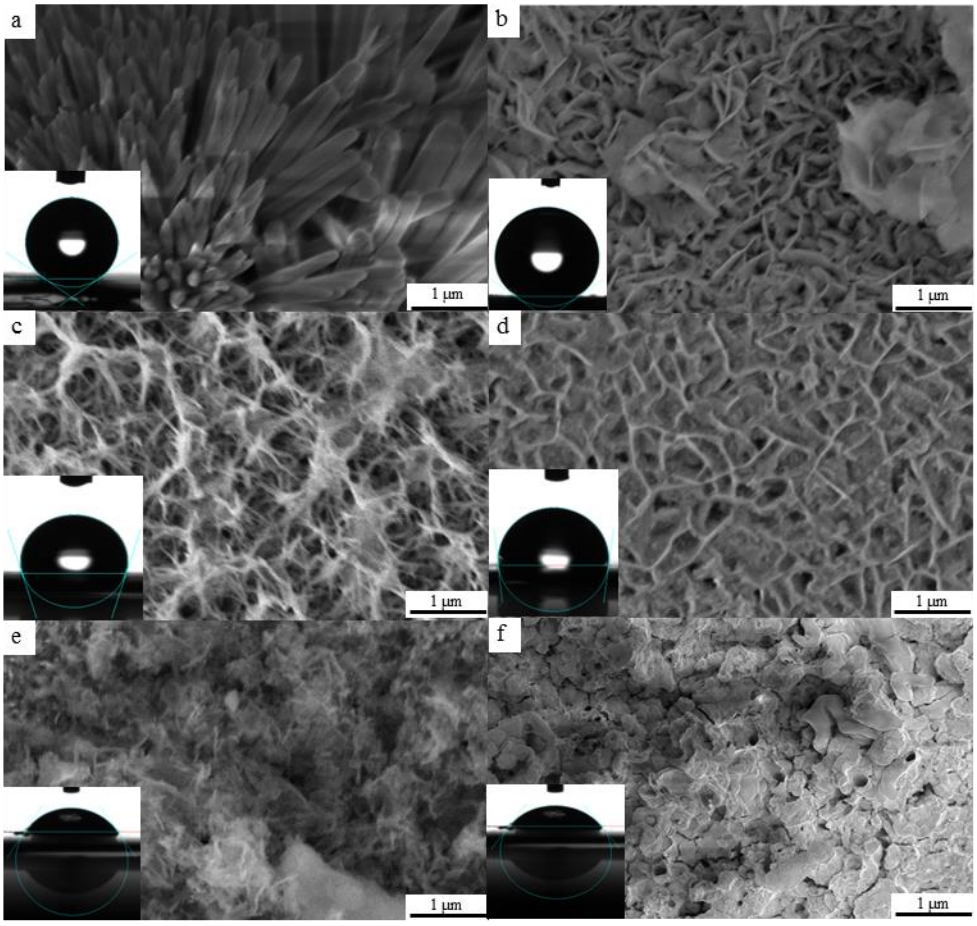


**Fig 6.** Contact angle and SEM micrographs of ZnO films exhibiting different wetting behaviours for different anodization conditions: a) $KHCO_3$ (1 M, 1 V, 1 min, 10 °C); b) $HNO_3$ (0.1 M, 1 V, 1 h, 10 °C); c) $H_2C_2O_4$ (0.1 M, 1 V, 1 h, 10 °C); d) $HNO_3$ (1 M, 40 V, 1 min, 10 °C); e) NaOH (0.1 M, 1 V, 1 h, 0°C); f) $H_2C_2O_4$ (0.1 M, 40 V, 1 h, 10 °C).

**Band Gap measurements**

The band gap of the ZnO films was measured through UV/Vis

absorption spectroscopy. No direct relationship was found between the intensity of the energy absorbed and the anodization conditions. ZnO films obtained using NaOH displayed the highest absorbance intensity (Figure S2) followed by films obtained with $HNO_3$; both films show a flower-like morphology with low surface density. On the other hand, ZnO films produced with $KHCO_3$, which have nanowire morphology, showed the lowest absorbance intensity, even though these were the thickest films produced in this study. These differences of absorbance intensity might also be attributed to scattering of the light by the nanostructures during the measurement.

The band gap exhibited by bulk ZnO is 3.37 eV.[23] Results obtained through this study showed band gap energies in the range of 3.27 to 3.50 eV. Films obtained with $H_2C_2O_4$ and $KHCO_3$ displayed the highest band gap energy; those films also showed the largest and densest nanostructures. Smaller, less dense nanostructures tend to have lower band gaps. Nonetheless, the differences in bad gap observed are within experimental error and therefore can be attributed to scattering effects due to the different film morphologies.

**Rational design guidelines for controlled formation of ZnO nanostructures via anodization**

**Morphology of ZnO surfaces**

The competition between formation and dissolution of ZnO is responsible for the formation of different types of nanostructures (Equations 1-5). These processes are strongly affected by the type of electrolyte and its concentration, current density, temperature and reaction time. Furthermore, as a multivariable process, any analysis must be done taking into account simultaneously all these variables. Figure 7a shows a 3D plot of different morphologies obtained with different electrolytes at different concentrations and, therefore, different pH, from data produced in this study and values obtained from literature. The colour of the dots represents the type of morphology. To simplify the analysis without omitting a third variable, Figure 7a was rotated (Figure 7b and 7c) to better visualise the distribution of the different morphologies for different pH, voltage and time. As discussed, temperature could not be included in this analysis due to the lack of detailed information in the literature.

The distribution of colours in Figure 7b and 7c confirms that pH and, therefore, electrolyte concentration, has the strongest influence over the type of morphology obtained during anodization. At low and high pH, 2D nanostructures (orange dots) are predominant. 1D nanostructures, such as nanowires and nanorods, have been obtained only in the range of neutral pH (green dots). Although the production of 1D and 2D nanostructures seems to be possible at different voltages and over different time periods, the majority of the studies have been focused on anodization at voltages lower than 20 V for time periods of less than 1 hour. Featureless films or films with un-structured rough surface (dark blue dots) have been obtained mainly at low pH and high voltage for different reaction times. This can be attributed to the dissolution mechanism dominating the ZnO nanostructures formation. In fact, anodization at high electrolyte concentration, high voltage and long periods of time, resulted in a featureless film for most electrolytes. Pitting and corrosion (light blue dots) are more common at low pH and high voltage.

3D interpenetrated nanostructures (red dots) can be obtained at any pH for medium-to-long times, as they are the result of a structuring of 1D or 2D nanostructures over time.

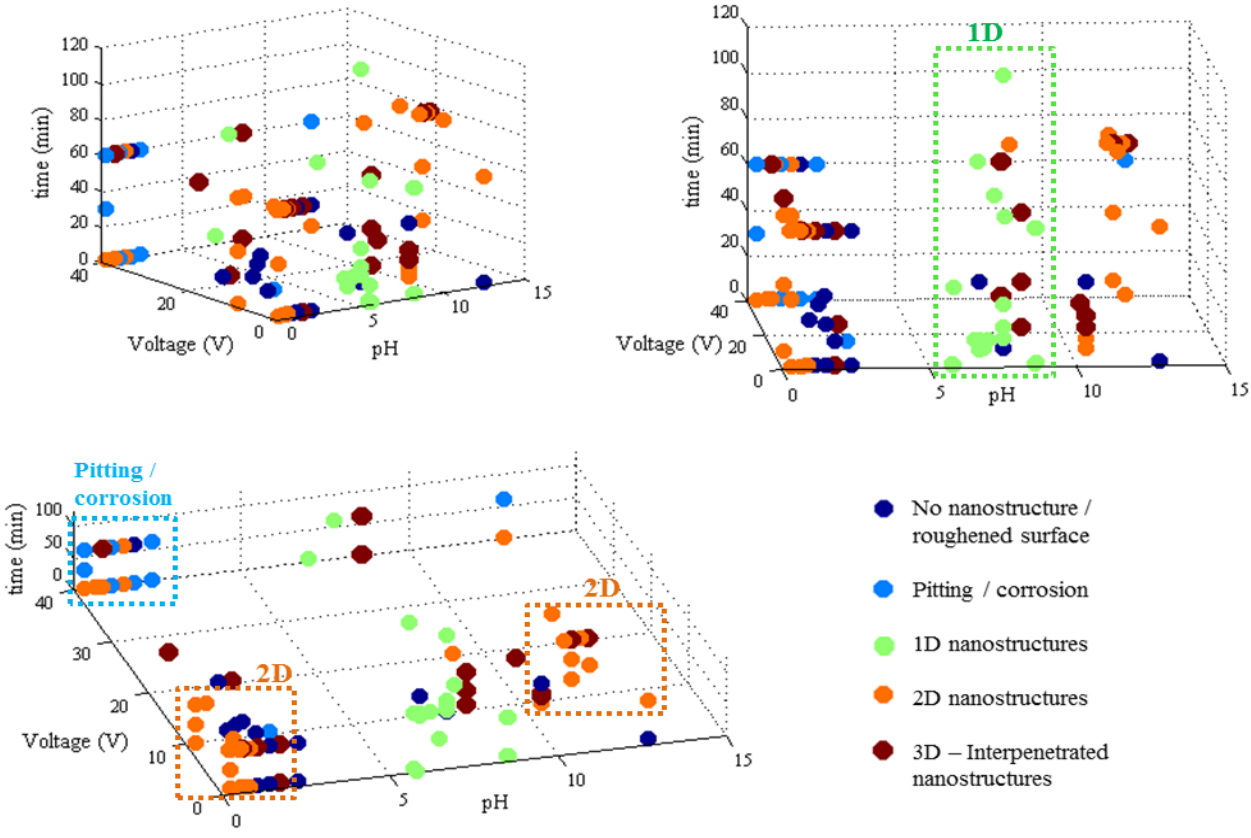


**Fig 7.** 3D plot of ZnO films obtained by anodization at different experimental conditions

### Contact Angle

The films' wetting behaviour is primarily related to the surface morphology, which is determined by the anodization conditions. For this analysis, data was plotted using a mirror-like plot, yielding the visualization of 8 possible combinations of experimental conditions (Figure 8a). This allows simultaneous comparison of the effect of voltage, pH, and temperature (Figure 8b); or voltage, pH, and time (figure 8c). Results suggest that a low pH and high voltage (40 V) favour the formation of super-hydrophobic surfaces (red dots) for all investigated temperatures.

Super-hydrophobic surfaces also predominate at neutral pH where the common morphology found is aligned 1D nanostructures, independent of the voltage, time or temperature. On the other hand, at low pH and low voltage (1 V) ZnO nanostructured surfaces tend to be more hydrophilic. The effect of time on the wetting behaviour of the ZnO nanostructures seems to be negligible at low voltage (1 V): By comparing, for each pH value, the lower middle row (Low V/High T) with the upper middle row of dots (Low V/Low T) similar values of contact angles are observed regardless of the anodization time. High voltage and longer times (top row) lead to super-hydrophobic surfaces being formed.

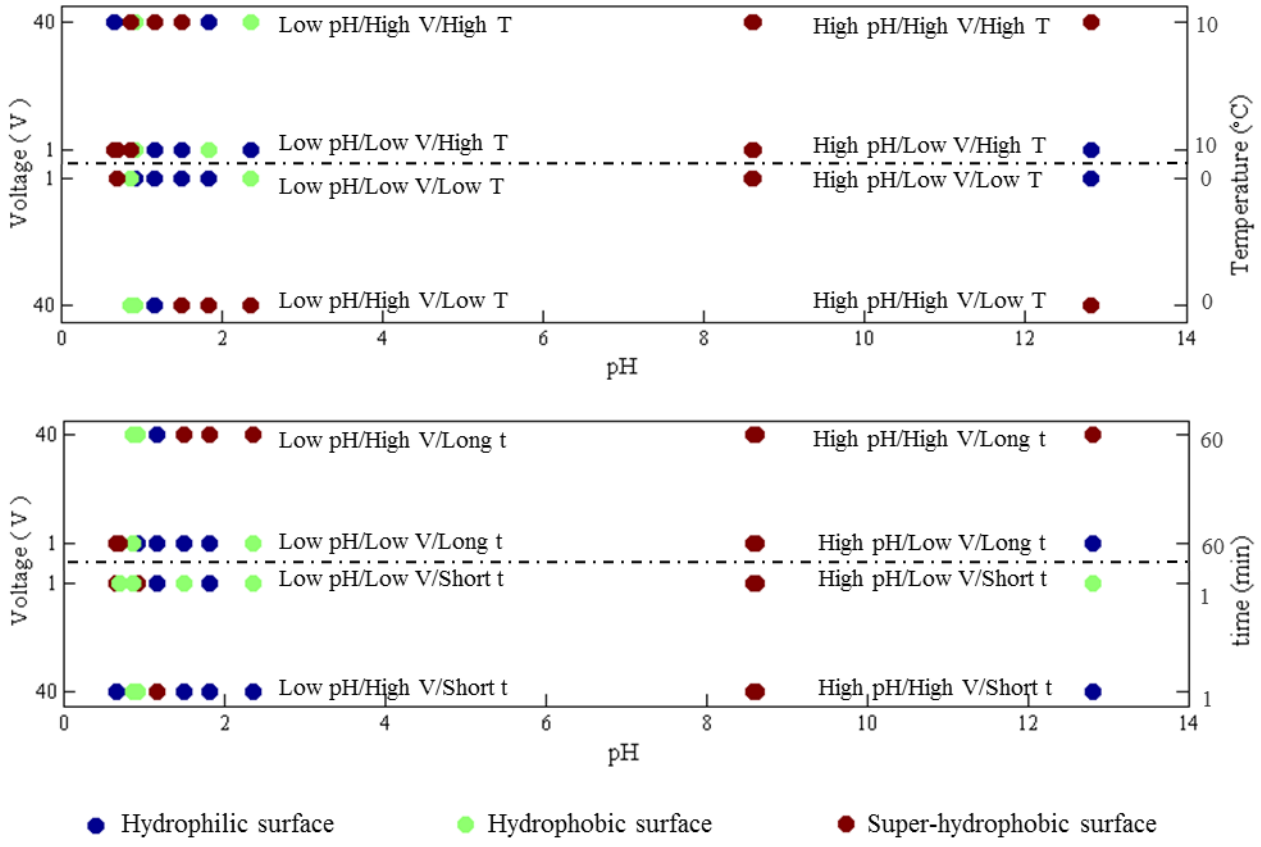


**Fig 8.** Wetting behaviour of ZnO films obtained by anodization at different experimental conditions.

## Conclusions

In conclusion, the morphology and properties of ZnO films obtained by anodization can be controlled through the synthesis conditions. The shape of the nanostructures is determined mainly by the type of electrolyte, while the nanostructure surface density increases with concentration, voltage and time. The latter experimental condition also determines the size of nanostructures, leading to the formation of 3D interpenetrated nanostructures once the nanostructures reach a certain length. The effect of temperature varies with the electrolyte, where acids at low temperatures reduce the formation of nanostructures considerably. Dense and well-aligned nanostructures with high aspect ratio display high contact angles, while low aspect ratios and less ordered surfaces show smaller contact angles, forming hydrophilic surfaces.

From these results the following design guidelines can be devised:

- 1D aligned arrays, usually (super-) hydrophobic, are mainly obtained at near neutral pH regardless of voltage and time.
- 3D arrays (hydrophobic and hydrophilic) are formed for long reaction times, regardless of the pH and the voltage.

- 2D arrays can be formed at low and high pH regardless of the voltage and time. However, 2D arrays formed at high pH display hydrophobic behaviour only at high voltage.
- The anodization conditions where corrosion and pitting are more common are low pH, high voltage and long-time reaction.

Detailed effects for each parameter combination can be found in Table S1.

## Acknowledgements

The authors acknowledge the Centre for Sustainable Chemical Technologies of University of Bath for funding support through a UK EPSRC (Grant No EP/G03768X/1) and COLCIENCIAS–Colombia for supporting this project via the award of Francisco Jose de Caldas Scholarship to ARC. DM is funded by a UK Royal Academy of Engineering Research Fellowship.

## Notes and references

[a] *Centre for sustainable Chemical Technologies of University of Bath , BA2 7AY, Bath, UK.*
[b] *Department of Chemistry of University of Bath, Bath, BA2 7AY, Bath, UK .*
[c] *Department of Chemical Engineering University of Bath, Bath, BA2 7AY, Bath, UK . Tel: +44 1225383961; E-mail: d.mattia@bath.ac.uk*

(1) Alhamed, M.; Abdullah, W. *Journal of Electron Devices* **2010**, *7*, 246-252.
(2) Kapustianyk, V.; Panasiuk, M. *J. of Phys studies* **2008**, *2*, 1-6.
(3) Wang, Y. C.; Leu, I. C.; Hon, M. H. *Journal of Crystal Growth* **2002**, *237-239*, 564-568.
(4) S. J. Pearton, C. J. *Zinc Oxide Bulk, Thin Films and Nanostructures: Processing, Properties and Applications*; Burlington Elsevier: London, 2006; pp. 339-370.
(5) X.-Y. Liu, C.-X. Shan, S.-P. Wang, H.-F. Zhao and D.-Z. Shen, *Nanoscale*, 2013, **5**, 7746-7749.
(6) Huang, Y. H.; Zhang, Y.; Gu, Y. S.; Bai, X. D.; Qi, J. J.; Liao, Q. L.; Liu, J. *J Phys Chem C* **2007**, *111(26)*, 9039-9043.
(7) Blossey, R. *Nature materials* **2003**, *2*, 301-6.
(8) Meng, Z.; Juan, Z. *Global Environmental Policy in Japan* **2008**, *12*, 1-9.
(9) Liu, X. *Journal of Applied Physics* **2004**, *95*, 3141.
(10) Yang, J. L.; An, S. J.; Park, W. I.; Yi, G.-C.; Choi, W. *Advanced Materials* **2004**, *16*, 1661-1664.
(11) Kawano, T.; Uchiyama, H.; Kiguchi, T.; Wada, S.; Imai, H. *Journal of the Ceramic Society of Japan* **2009**, *117*, 255-257.
(12) Basu, P. K.; Saha, N.; Maji, S.; Saha, H.; Basu, S. *Journal of Materials Science: Materials in Electronics* **2008**, *19*, 493-499.
(13) Huey-Shya, G.; Adnan, R.; Farrukh, M. *Turk J Chem* **2011**, *35*, 375-391.
(14) Wu, X.; Lu, G.; Li, C.; Shi, G. *Nanotechnology* **2006**, *17*, 4936-4940.
(15) He, S.; Zheng, M.; Yao, L.; Yuan, X.; Li, M.; Ma, L.; Shen, W. *Applied Surface Science* **2010**, *256*, 2557-2562.
(16) Kuan, C. Y.; Chou, J. M.; Leu, I. C.; Hon, M. H. *Electrochemistry Communications* **2007**, *9*, 2093-2097.
(17) Kim, S. J.; Choi, J. *Electrochemistry Communications* **2008**, *10*, 175-179.
(18) Wang, Z. *Materials today* **2004**, 26-33.
(19) Farrukh, M. A.; Thong, C.-K.; Adnan, R.; Kamarulzaman, M. A. *Russian Journal of Physical Chemistry A* **2012**, *86*, 2041-2048.
(20) Kim, S. J.; Lee, J.; Choi, J. *Electrochimica Acta* **2008**, *53*, 7941-7945.
(21) Basu, P. K.; Bontempi, E.; Maji, S.; Saha, H.; Basu, S. *Journal of Materials Science: Materials in Electronics* **2009**, *20*, 1203-1207.
(22) Huang, G. S.; Wu, X. L.; Cheng, Y. C.; Shen, J. C.; Huang, A. P.; Chu, P. K. *Applied Physics A* **2006**, *86*, 463-467.
(23) Srimala Sreekantan, Lee Ren Gee, Z. L. *Journal of Alloys and Compounds* **2009**, *476*, 513-518.
(24) Wu, X.; Lu, G.; Li, C.; Shi, G. *Nanotechnology* **2006**, *17*, 4936-4940.
(25) Kim, Y.-T.; Park, J.; Kim, S.; Park, D. W.; Choi, J. *Electrochimica Acta* **2012**, *78*, 417-421.
(26) Zhudong Hu, Qing Chen, Zhen Li, Yuan Yu, L.-M. P. *journal of Physical Chemistry C- J PHYS CHEM C* **2010**, *114*, 881-889.
(27) Sakai, M.; Kono, H.; Nakajima, A.; Zhang, X.; Sakai, H.; Abe, M.; Fujishima, A. *Langmuir : the ACS journal of surfaces and colloids* **2009**, *25*, 14182-6.
(28) Feng, X.; Feng, L.; Jin, M.; Zhai, J.; Jiang, L.; Zhu, D. *Journal of the American Chemical Society* **2004**, *126*, 62-3.
(29) Zhang, Z.; Chen, H.; Zhong, J.; Saraf, G.; Lu, Y. *Journal of Electronic Materials* **2007**, *36*, 895-899.
(30) Zhang, J.; Huang, W.; Han, Y. *Langmuir : the ACS journal of surfaces and colloids* **2006**, *22*, 2946-50.
(31) Han, J.; Gao, W. *Journal of Electronic Materials* **2008**, *38*, 601-608.
(32) Zeng, B. H.; Duan, G.; Li, Y.; Yang, S.; Xu, X. *Advanced Functional Materials* **2010**, *20*, 561-572.
(33) Wang, F.; Liu, R.; Pan, A.; Cao, L.; Cheng, K.; Xue, B.; Wang, G.; Meng, Q.; Li, J.; Li, Q.; Wang, Y.; Wang, T.; Zou, B. *Materials Letters* **2007**, *61*, 2000-2003.
(34) Yi, S.-H.; Choi, S.-K.; Jang, J.-M.; Kim, J.-A.; Jung, W.-G. *Journal of colloid and interface science* **2007**, *313*, 705-10.
(35) Cassie, A.B.D., Baxter, S. *Transactions of the Faraday Society* **1944**, *40*, 546-551.
(36) Wenzel, R. N. *Industrial and Engineering Chemistry* **1936**, *28*, 988.